Trans. JSASS Aerospace Tech. Japan
Vol. 12, pp. 11-19, 2014

Discharge Observation on Antenna Surface Radiating High-power Microwaves in Simulated Space Environment

By Hyounggwan WOO, [1)] Arifur R. KHAN,[2)] Hirokazu MASUI,[2)] Mengu CHO,[2)]
Takehiro MIYAKAWA,[3)] and Tatsuhito FUJITA[3)]

[1)]*Department of Electric and Electronic Engineering, Kyushu Institute of Technology, Kitakyushu, Japan*
[2)]*Department of Applied Science for Integrated System Engineering, Kyushu Institute of Technology, Kitakyushu, Japan*
[3)]*Advanced Mission Research Group, Japan Aerospace Exploration Agency, Tsukuba, Japan*

(Received December 26th, 2012)

The space solar power system (SSPS) transfers enormous amounts of electrical energy through microwaves. When high-power microwaves are irradiated from an antenna in a LEO plasma environment, there is a concern about discharge caused by interaction between the plasma and the microwaves. There has been no experimental observation of such an interaction phenomenon. Verification experiments are essential for SSPS to become a reality. We examine whether discharge or related phenomena occur or not on patch antennas under various conditions in the laboratory. We verify the hypothesis of discharge inception that the discharge is caused by multipactoring and breakdown of the outgas product. We compute the minimum electric field for the discharge inception.

Key Words: SSPS, Multipactoring, Total Electron Emission Yield, Patch Antenna, Microwave

1. Introduction

The power demand on the Earth is growing exponentially and the associated environmental consequences are becoming significant. Therefore, there are expectations that the space solar power system (SSPS) [1,2)] can become one of the solutions to the problem. SSPS transfers enormous amounts of electrical energy in the form of microwaves. Before commercialization of SSPS, we must go through various technological demonstrations in orbit. Although the commercial SSPS is envisioned at geostationary orbit (GEO) to supply the continuous power to the ground, the first demonstration of the wireless power transmission between space and the ground will be done using a satellite in low Earth orbit (LEO) for its easy access to the orbit and short distance. The main purpose of the orbital demonstration is to steer the beam power to a specific point on the ground using a phased array antenna. The satellite will be surrounded by ionospheric plasma whose density ranges from 10^{10} to 10^{12}m^{-3}, six orders of magnitude higher than the plasma density at GEO. A severe interaction between the surrounding plasma and the antenna is envisioned. [3)] Therefore, before the experiment in LEO, the interaction phenomena must be studied on the ground.

The purpose of this study is to carry out laboratory experiments to observe the discharge phenomena occurring on the antenna surface when it emits strong microwaves in a plasma environment similar to the LEO. We anticipate that the discharge occurs on the antenna surface due to multipactoring and RF gas breakdown. The first purpose of the experiment is to see how the discharge occurs and second to study why it occurs. In the present study we choose a circular patch antenna as a test sample because it is a strong candidate for the phased array antenna of the SSPS demonstration satellite as well as to the final commercial SSPS, owing to its simplicity and ease of manufacturing. In the case of the commercial SSPS, which provides 1 GW power to the ground, each patch antenna is distributed in 5.17 cm wavelength intervals that emit power of 2.5 W.

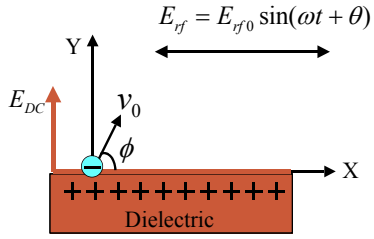

Fig. 1. Schematic of a single-surface multipactor in a parallel rf and normal DC electric fields.

Multipactor discharge is a ubiquitous phenomenon observed in a multitude of devices that employ microwaves. [4)] It may occur when a metallic gap or a dielectric surface is exposed to an AC electric field under some favorable conditions, and its avoidance has been a major concern in development of high-power microwave sources, RF accelerators and space-based communication systems. [4-7)] The underlying mechanism behind the

multipactor discharge is an avalanche caused by secondary electrons. The discharge can take place on a single surface or between two surfaces. [8] In this experiment, we assume the single-surface multipactor shown in Fig. 1.

At the first stage, a stray electron gains energy from the RF electric field (E_{rf}) that is parallel to the dielectric surface. If this electron collides with the surface of the dielectric, then one or more secondary electrons are freed from the surface. At the second stage, when the secondary electrons leave the dielectric, a net positive charge is left on the surface of the dielectric. This net positive charge produces a DC electric field (E_{dc}) normal to the dielectric surface. This E_{dc} causes the trajectory of the electron to be bent back towards the dielectric. If these electrons gain enough energy from E_{rf}, they can produce more secondary electrons when they hit the surface and the multiplication process is initiated. At the third stage, a half RF cycle later, the E_{rf} reverses its direction, leading to severe local heating of the dielectric by electrons. Synchronism between the RF field and the orbits is not critical in the single-surface multipactor because in the half RF cycle there are numerous impacts of multipactor electrons. [9] The fundamental mode of the multipacting mechanism of high-frequency gaseous breakdown, also known as the secondary electron resonance mechanism, is postulated on 1/2-cycle electron transit time between electrodes, and electron multiplication by secondary electron emission at the electrode surface. [10]

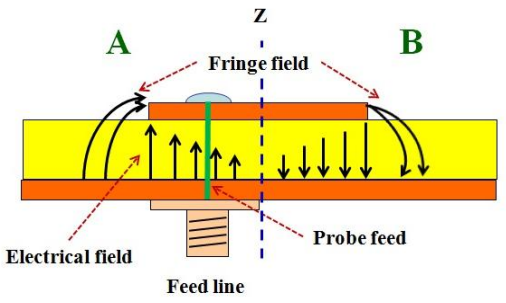

Fig. 2. Nature of electric field when a patch antenna radiates microwaves.

A patch antenna with its electric field is shown in Fig. 2, when it radiates electromagnetic waves. The electromagnetic energy is first guided or coupled to the region under the patch, which acts like a resonant cavity with open circuits on the sides. Some of the energy leaks out of the cavity and radiates into space, resulting in an antenna. The electric field is zero at the center of the patch, mostly positive at one side (B region), and mostly negative on the opposite side (A region). It should be mentioned that the positive and negative continuously change the side according to the instantaneous phase of the applied signal. The electric field does not stop abruptly at the patch's periphery as in a cavity; rather, the fields extend the outer periphery to some degree. These field extensions are known as fringing fields and cause the patch to radiate. We can calculate the threshold electric field from radiation power.

This paper consists made of five sections. The second section describes the experimental setup and procedure. The third section reports the experimental results. The fourth section compares a hypothesis about the discharge inception mechanism against the experimental results. The fifth section concludes the paper with suggestions for future works.

2. Experimental Setup

2.1. Experimental system

Figure 3 shows a schematic of the experimental setup. A cryogenic pump (ULVAC) backed by two rotary pumps evacuates the chamber up to a pressure of 1×10^{-5}Pa. The chamber has a square shape with dimensions of 115 × 100 × 75 cm. To study the discharge on the surface of patch antennas, it is placed inside the vacuum chamber, connected through a coaxial feed-through to the microwave generator (MMG-604V, Microelectronic) placed outside of the chamber able to oscillate with a fixed frequency of 5.8 GHz±15 MHz, and generate power from 0～400 W. The microwave is introduced to the antenna through the waveguide and coaxial cable that is connected by a coaxial adapter. For safety reasons the entire vacuum chamber with all it accessories (plasma source and its power supplies, etc.) are kept inside the microwave protective shield.

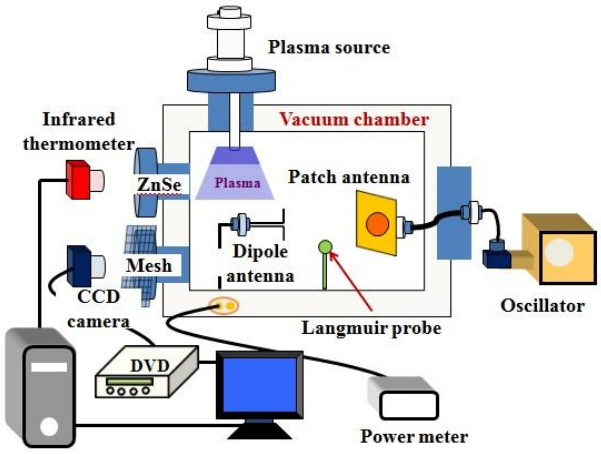

Fig. 3. Experimental system.

The input power is measured by monitoring the anode current of the magnetron and using a calibration table provided by the manufacturer.

The radiated power from the patch antenna is monitored by a dipole antenna, placed 10 cm away from the source, and measured by a power sensor (HP8481B) and a power

meter (HP437B, Agilent) from the chamber outside. We place a CCD camera (MTV-6368ND) and an IR thermometer (PI-160, Optris) to detect the light emission during discharge and monitor the temperature distribution over the antenna surface from the chamber outside. To protect the camera and the thermometer from interference of the microwaves, we cover the viewports (glass and ZnSe) with a metallic mesh. The thermometer can measure temperature from 0 to 275℃. The chamber pressure, the radiated power from the antenna and the input power to the antenna are recorded simultaneously by a computer connected through a data acquisition (DAQ) system running a Labview program. A RF excited radical plasma source and RF generator (T857-2, CREATE) are placed on the top of chamber.

A Langmuir probe is installed inside the chamber to measure the plasma parameters, such as density, electron temperature, etc., shown in Fig.4. The Langmuir probe is located at a distance of 10 cm from the center of the patch antenna. (It is 9.8 cm in the off-axial direction from the line connecting the dipole antenna and the patch antenna and 2 cm from the plane containing the patch antenna.) We measure the plasma density inside the chamber, which is varied from 10^{11} to 10^{13}[1/m^3] with the electron temperature between 3 and 5.5 eV that is controlled by the RF power and the Ar gas flow rate. During the plasma experiment, the background pressure is approximately 2.6×10^{-2} Pa.

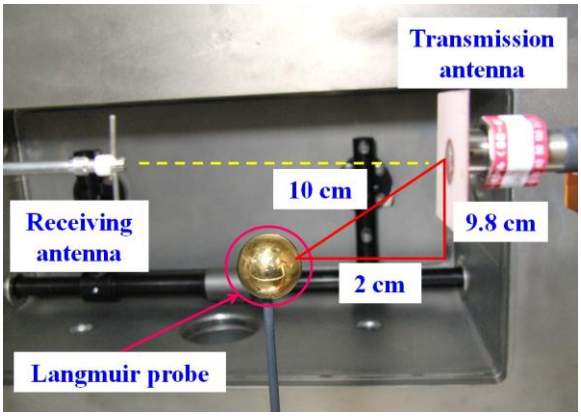

Fig. 4. Transmission (patch) and receiving (dipole) antennas.

2.2. Patch antenna

A microstrip patch antenna is made of a dielectric substance sandwiched by conductors of identical type. The front conducting layer acts as the radiating face connected to the microwave cable, whereas the opposite conducting layer acts as reference ground. The radiating face may be rectangular or circular with various dimensions. The basic structure of the microstrip patch antenna is shown in Fig. 5. The antenna patch and the ground of this antenna used in this experiment are made of copper. The thickness and radius of patch are 0.02 and 6.8 mm, respectively. The thickness of glass epoxy as dielectric is 0.8 mm.

The typical electric field near the circular patch can be estimated following Refs. 11), 12) and 13) where the circumferential wall of the cavity is replaced by an equivalent magnetic current density radiating in free space. Based on the cavity model, the normalized electric fields of the z direction within the cavity for the cosine azimuthal variations can be written assuming TM_{11} mode as follows, [11)]

$$E_z = E_0 J_1(k\rho)\cos(n\phi) \tag{1}$$

where the coordinate ρ is used to represent the fields within the cavity while $J_m(x)$ is the Bessel function of the first kind of order m. ϕ' is the azimuthal angle along the perimeter of the patch, E_z is the electric field across the gap at ρ', k is the propagation constant in the dielectric and E_0 is the electric field across the gap given by [12)]

$$V_0 = hE_o J_1(ka) \quad (\text{at } \phi=0) \tag{2}$$

where V_0 is the voltage across the gap, h is the substrate thickness and a is the radius of the patch.

The electric field due to the radiated power of the circular microstrip patch antenna can be computed based on the radiated power expressed as [13)]

$$P_{rad} = |V_0|^2 \frac{\alpha^2}{960}\int_0^{\pi/2}\left[J_{02}'^2 + \cos^2\theta J_{02}^2\right]\sin\theta d\theta \tag{3}$$

where $\alpha=k_0a$ and k_0 is the free space phase constant ($k_0=2\pi f_r/v_0$, $v_0=3\times10^{10}$cm/s) and θ is the elevation angle ($0^\circ \le \theta \le 90^\circ$). J'_{02} and J_{02} are given by

$$\begin{aligned} J'_{02} &= J_0(k_0 a\sin\theta) - J_2(k_0 a\sin\theta) \\ J_{02} &= J_0(k_0 a\sin\theta) + J_2(k_0 a\sin\theta) \end{aligned} \tag{4}$$

For f_r=5.8 GHz and a= 6.8 mm, the integral in Eq.3 is approximately 1.0. Assuming no loss of the incident power to the radiated power from patch antenna, we have P_{rad} as a given input power value. Then V_0 is calculated from Eq. (3). We can calculate the electric field of the perimeter of the patch, E_z, from Eqs. (1) and (2). Table 1 lists the results of the relationship between the maximum electric field and voltage at the edge of the antenna as a function of incident power. We used h=0.8 mm.

Table 1. Electric field between the patch and the ground as a function of incident power.

Incident power, P_{rad} [W]	V_0 [V]	E_z [x10^{5}V/m]
5	84	1.0
10	118	1.5
15	145	1.8
20	167	2.1
25	187	2.3
30	205	2.6
35	221	2.8
40	237	3.0
45	251	3.1

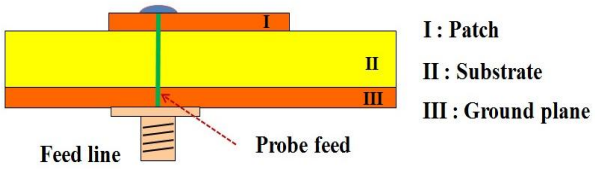

(a) Basic structure of the microstrip patch antenna

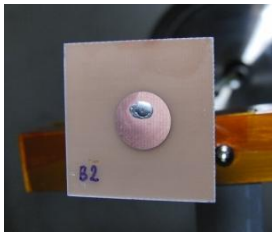

(b) Photograph of patch antenna having FR4 (glass epoxy) as dielectric

Fig. 5. 5.8 GHz microstrip patch antennas.

2.3. Experiment procedure

Microwaves are transmitted to the patch antenna through the waveguide and the coaxial cable. A calibrated dipole antenna connected to a spectrum analyzer (R3132, ADVANTEST) confirms the radiation frequency. The dipole antenna also measures the radiated power from the patch antenna. Both radiated and received power are measured by the power meter and recorded to the computer in a time domain. The microwave input power is increased by a 5 W step keeping each value for five minutes to check whether discharge occurs or not. This process is continued until the discharge is detected by a CCD camera or sudden pressure rise. In the case of the plasma environment, the discharge is confirmed by the CCD camera only.

As the chamber walls reflect the electromagnetic waves, the dipole antenna cannot measure the radiated power correctly. Before the main experiment we use a electromagnetic wave absorber for test of the received power by the dipole antenna. As a result, the received power is 2~3 times higher than that of the case with the absorber. It is, however, not our intention to measure the radiated power correctly. In this experiment, the dipole antenna is used to check whether the radiated power increases or decreases when the discharge occurs on the patch antenna. Therefore, the experiments are conducted without an electromagnetic wave absorber in the vacuum chamber. This is also to keep the vacuum environment clean.

2.4. Experiment condition

Various cases are tested in the vacuum chamber, such as LEO equivalent plasma and excess degassing to verify their effects on the discharge on the patch antenna. Plasma is generated by Ar gas under the oscillation of 13.56 MHz. Non-conductive room temperature vulcanized silicon adhesive (RTV-S691) is painted to promote degassing from the surface. RTV-S691 is chosen as it could degass significantly by heating. Without the adhesive, the glass epoxy substrate alone is not enough to cause discharge within the power level tested. There are two types of painting, ring and disk. The disk type (Fig.6(b)) is tried first. However, no discharge is observed. The temperature measured by the thermograph indicates higher temperature at the rim of the patch. Therefore, we paint the adhesive along the rim in a ring shape (Fig.6(c)). Table 2 lists the condition of each experiment carried out with identical patch antennas made of FR4.

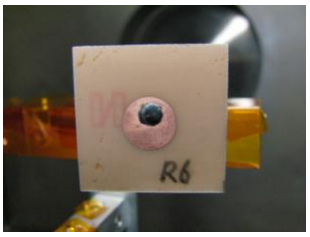

(a) Normal patch antenna (FR4 as dielectric)

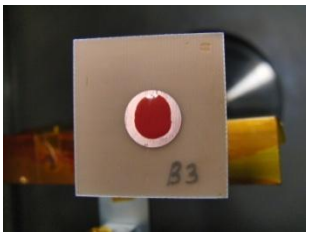

(b) Disk type RTV painted on patch antenna

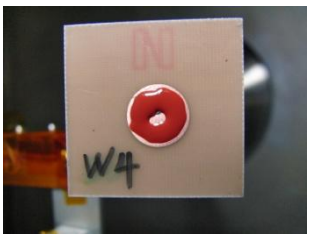

(c) Ring type RTV painted on patch antenna

Fig. 6. Patch antenna with different preparations.

Table 2. Experimental condition for patch antennas (FR4 type).

	Pressure	Vacuum only	Plasma density [m^{-3}]		Painted (RTV)	
	10^{-5} [Pa]		10^{11}	10^{13}	Ring	Disk
A	3.4	○				○
B	3.4	○			○	
C	2,700		○		○	
D	2,800			○	○	
E	2,600		○			○
F	3,200			○		
G	2,800		○			
H	2.2	○				
I	2.4	○				
J	2,600		○			

3. Results

After setting the patch antenna, the microwave power is raised manually in 5 W steps after every five-minute interval as shown by the blue line (right y-axis) in Fig.7 (top). The left y-axis (red line) shows the patch antenna radiated power received by the dipole antenna. As we raise the microwave power, the following events are observed. As an example we show the temporal profile of the received power, the chamber pressure and the sample temperature for the case of sample B in Fig. 7. The temperature plotted here is the maximum value in the measurement area of 3 ×2.5 cm centered around the patch.

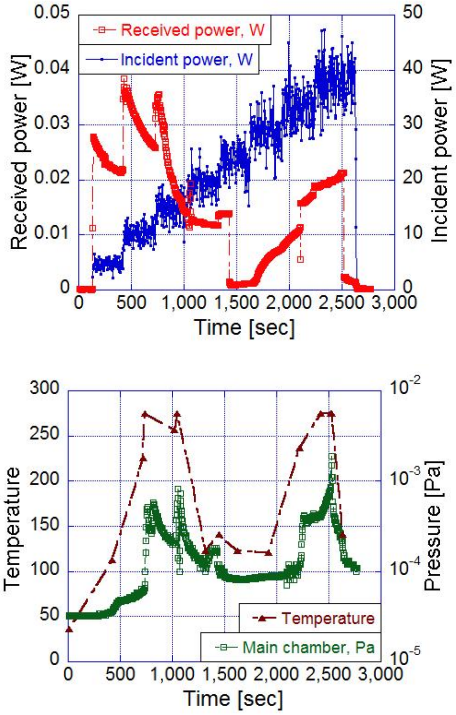

(a) Sample B

Fig. 7. Variation of received power and pressure according to the incident power and temperature in vacuum only.

1. As the microwave power is turned on, the received power at the dipole antenna instantaneously increases and decays. This decay is probably because the patch antenna temperature keeps increasing while we keep the microwave power steady and the antenna shape deforms slightly and the permittivity changes due to the temperature increase.
2. The received power shows a step-wise increase as the microwave power is increased by 5 W from 5 W to 10 W. The pressure slightly increases as the temperature increases promote the out-gassing from the antenna surface.
3. As the incident power is increased from 10 to 15 W, the temperature exceeds the limit of the thermometer (275℃) showing a very rapid increase. In Fig. 8 a thermograph image is shown. It should be noted that the temperature distribution is not uniform. The pressure jumps by one order of magnitude. After this jump, the received power decreases and it is even lower than the value received at the incident power of 5 W. This suggests that the antenna is irreversibly damaged.

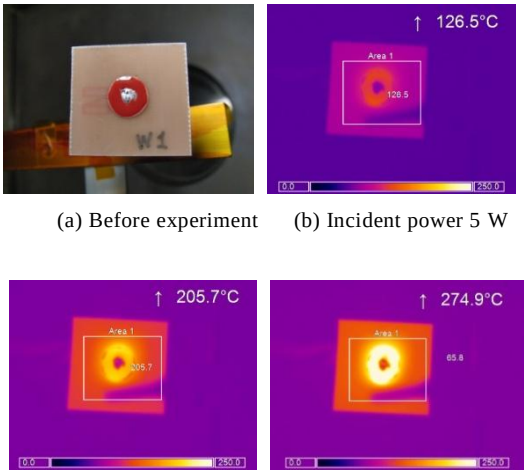

(a) Before experiment (b) Incident power 5 W

(c) Incident power 10 W (d) Incident power 15 W

Fig. 8. Image of the thermography of sample B.

Figure 9 shows photographs of samples (Fig.9(d) is different from sample B) that are removed from the chamber after this phenomenon. We can clearly see that the antenna is physical damaged at the edge and the surface of the patch. Fig.9(b) shows an enlarged photograph near the edge of the antenna. Melted char is visible around the edge and covers the copper. We see no clear deformation of the copper, but the dielectric property of the FR4 substrate is inevitable. The char is not conductive as far as measured by a tester. The reason of the drop of the received power is due to either the change of the radiation pattern or the increase of the reflection power.

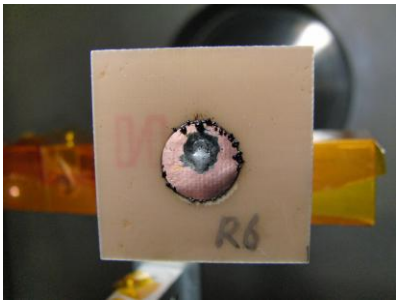

(a) Normal patch antenna

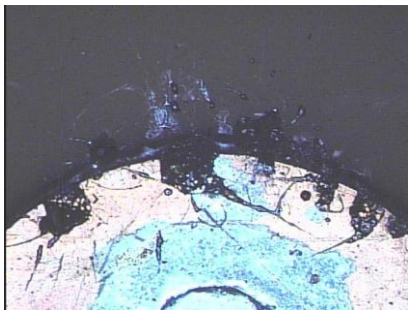

(b) Enlarged photograph near the edge of (a)

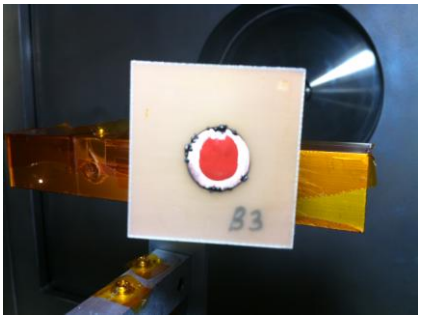

(c) Disk type RTV painted on the patch antenna

(d) Ring type RTV painted on the patch antenna

Fig. 9. Photograph of antenna removed from the chamber after the temperature rise.

For other antennas, this change of the received power occurs whenever the antenna surface temperature exceeds 275℃. It should be noted that the exact temperature is unknown in excess of 275℃, the temperature limit of the thermometer. The glass transition temperature of FR4 is generally approximately 150℃. Therefore, although the temperature of 275℃ is mostly observed on the copper surface, it is high enough to cause irreversible damage to the antenna. When the experiments are done without the plasma, we are always able to observe the jump of the background pressure associated with the temperature rising beyond 275℃. When the plasma source is operating, the background pressure is too high to notice the pressure change. Practically, once this phenomenon occurs, the antenna no longer functions as it is designed. Therefore the threshold condition of this phenomenon provides a practical limit on the microwave power injected to the antenna element.

4. We keep increasing the microwave power. The received power shows complicated variation. The temperature dropps to below 150℃ and again we observe the received power increasing. As the power is increased to 40 W, we observe a bright emission from the sample surface as shown in Fig. 10. When we observe the light emission, the temperature is again off the scale and the pressure increase is far more than the previous pressure increase at 15 W (see near 2,500 sec in Fig. 7). The received power abruptly drops to a near zero value. We think this is discharge. At the beginning of discharge, there is a weak light at the patch's periphery. Later, it is gradually intensified as the time goes on. For other samples, we raise the microwave power while we observe the discharge light emission. The light emission becomes brighter as we increase the power. The dense plasma generated by the discharge absorbs the incident microwave and emits the light. At the same time, the discharge plasma heats the antenna surface. The antenna surface material is evaporated and the chamber pressure jumps. Figure 11 shows a photograph of sample B after the experiment. We can see extensive damage at the edge of the antenna surface.

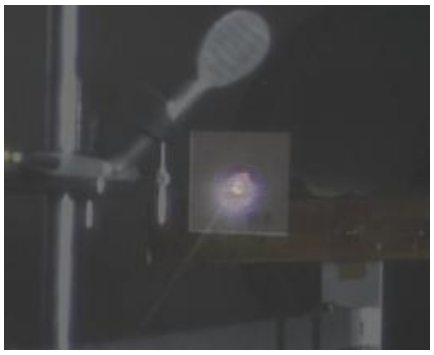

Fig. 10. Discharge emitting light on the surface of the patch antenna.

Fig. 11. Photograph of sample B after the experiment.

In this paper, we define the threshold values of the two phenomena. The first one is the rapid increase of the temperature exceeding 275℃. This phenomenon is associated with the irreversible change in the received power by the dipole antenna and the abrupt pressure jump (when the plasma source is not operating). We call this phenomena "out-gassing" in the present paper. The second one is the bright light emission on the antenna surface. This phenomenon is associated with the abrupt drop of the received power by the dipole antenna and the abrupt pressure jump. We call this phenomenon "discharge" in the present paper. Table 3 lists the microwave input power when these two phenomena are observed for the various experimental conditions. In the table, "None" means that the discharge is not observed up to 45 W of the microwave input power. As the sample is damaged after each experiment, a new sample is used. The appendix shows the temporal profile of the other samples.

Table 3 shows that we can observe the out-gassing on the ring type RTV painted antenna when the incident power is 15 W. The disk type RTV painted antenna shows the out-gassing under 15 to 20 W incident power. For normal patch antennas (samples K and L) without any additional features, such as RTV paint or the plasma environment, the out-gassing is observed only under 25 W incident power.

Table 3. Comparison of discharge phenomena at different environments and FR4 substrates.

Sample	Condition	Incident power [W]	
		Out-gassing	Discharge
A	V, DR	15	None
B	V, RR	15	40
C	P, RR	15	20
D	P, RR	15	None
E	P, DR	20	15
F	P	20	None
G	P	20	None
H	V	25	None
I	V	25	None
J	P	25	None

* V : Vacuum only, P : Plasma environment,
DR : Disk type RTV, RR : Ring type RTV.

4. Discussion

Figure 12 shows the discharge inception mechanism we consider. When the power is supplied to the patch antenna, an electron is accelerated by the fringe electric field and hits the surface of the substrate (Fig. 12(a)). The impact induces the emission of secondary electrons. Figure 13 shows the total secondary electron yield of the glass epoxy laminate board. The total secondary electron yield is measured by the secondary electron yield measurement facility at Kyushu Institute of Technology.[14] The first crossover of unity of the secondary electron yield curve is less than 25 eV. If the incident electron is accelerated to the energy above the first crossover, one incident electron can emit more than one secondary electron (Fig. 12(b)). The secondary electrons are emitted and accelerated by the RF field. Note that the electric field has a component parallel to the antenna surface. As Ref. 9) suggests, the vertical DC electric field attracts the electrons. Multiplication of the secondary electron occurs when their incident energy exceed the first crossover (Fig. 12(c)). As the number of electrons increases, the heat input to a localized area by the electrons increases and the temperature increases locally (Fig. 12(d)). The temperature increase leads to desorption of gas from the surface. The desorption is also caused by the electron impact (Fig. 12(e)). Electron multiplication proceeds further as there is contribution due to ionization of the desorbed gas (Fig. 12(f)). At one point, the localized temperature exceeds the melting temperature of the dielectric. The glass transition temperature of FR4 is approximately 150℃. The gas density jumps due to evaporation. The high temperature causes irreversible change to the antenna. This is the "out-gas" phenomena observed in the experiment. As the electron multiplication and out-gassing proceeds further, the localized gas density becomes high enough to have microwave gas breakdown. This is the "discharge" phenomena observed in the experiment.

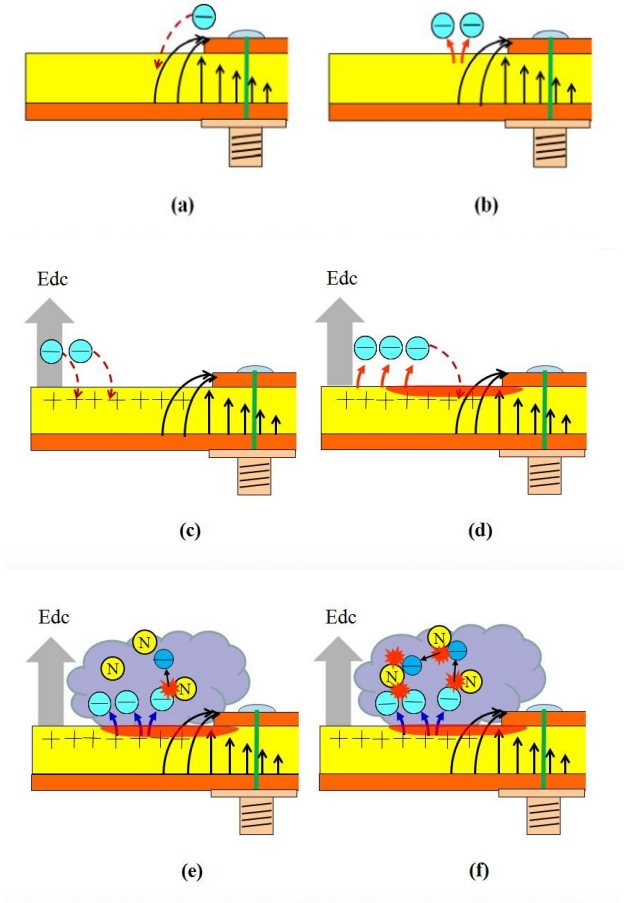

Fig. 12. Schematics of discharge formation.

Let v_{max} be the maximum velocity of electron, E_1, the first crossover of secondary electron emission yield. Only when the primary electron energy is higher than E_1, more secondary electrons can be generated.

$$E_{impact} = \frac{1}{2} m (v_{\max})^2 > E_1 \qquad (5)$$

where

$$v_{\max} = \frac{eE}{m\omega} \ ,$$

E_1=25 [eV] (on the glass epoxy substrate) gives v_{max} and should be larger than 3.0×10^6 (m/s).

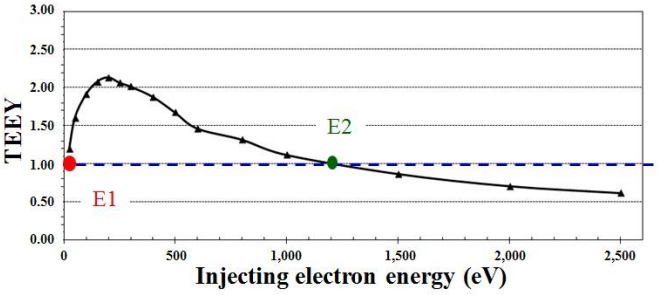

Fig. 13. Total electron emission yield (TEEY) of glass epoxy laminate board.

To accelerate an electron to energy of 25 eV within a half period of the RF frequency (5.8 GHz), we need the RF electric field of 6.2×10^5 V/m. The threshold incident power is different for each condition. However, the fringe electric field at 15 W is 1.8×10^5 V/m and 40 W is $3.0\text{x}10^5$ V/m (see Table 1). The value in Table 1 assumes the antennas are symmetric. As the patch antennas used in the experiments are asymmetric, the maximum radiation field is expected to be higher than the values in Table 1, [11] in the order of 10^5V/m or larger. They are within the same order of magnitude. This agreement is encouraging considering the primitive nature of discussion based only on energy.

5. Conclusions

On-orbit demonstration of SSPS is being planned onboard a small satellite in LEO. Radiation of intense microwaves in the dense LEO plasma raises serious concern over the interaction between the microwave and the plasma, such as discharge on the antenna surface.

To investigate the possible phenomena in orbit, we performed a laboratory experiment where we emitted 5.8 GHz microwaves via a patch antenna in a vacuum chamber filled with plasma. Until now, the bright light emission due to discharge was confirmed in the incident power range of 20-40 W. The patch antenna temperature was observed to exceed 275 ℃.

Hereafter, we need to investigate more about the operating conditions in the orbit by ground experiments as accurately as possible. We will carry out experiments with several other substrate materials of antenna which can be used in the actual SSPS.

References

1) Mori, M. : SSPS review in NASDA, 4th SPS Symposium, 2001, pp.121-125. (in Japanese)
2) Kobayashi, T. : Commercialization of SSPS and Activities of USEF, 5th SPS Symposium, 2002, pp.126-130. (in Japanese)
3) Cho, M. : Discharge Phenomena on a Solar Array under RF Irradiation, Technical Report of IEICE SPS, 2006-06.
4) Vaughan, J. R. M. : Multipactor, *IEEE Trans. Electron Devices*, **35** (1988), p.1172.
5) R. A. Rimmer, High Power Microwave Window Failures, Ph.D. Dissertation, Univ. Lancaster, U.K. 1988.
6) S. Yamaguchi, Y. Saito, S. Anami, and S. Michizono, : Trajectory Simulation of Multipactoring Electrons in an S-band Pillbox RF Window, *IEEE Trans. Nucl. Sci*., **39** (1992), p.278.
7) N. Rozario et al : Investigation of Telstar 4 Spacecraft Ku-band and C-band Antenna Components for Multipactor Breakdown, *IEEE Trans. Microwave Theory Tech*., **42** (1994), p.558.
8) R.A.Kishek, : Multipactor Discharge on Metals and Dielectrics : Historical Review and Recent Theories, *Phys. Plasmas*, **5**,5 (1998), pp.2120-2126
9) Lay-Kee Ang, Y. Y. Lau, Rami A. Kishek, and Ronald M. Gilgenbach, : Power Deposited on a Dielectric by Multipactor, *IEEE Trans. Plasma Sci*., **26**, 3 (1998), p.290.
10) E. L. Nichols, : Multipacting Modes of High-Frequency Gaseous Breakdown, *The Physical Review*, (1893). pp.681-685
11) Bancroft R. : Microstrip and Printed Antenna Design, 2nd ed., SciTech Publishing, Raleigh, NC, 2009, Chap.3.
12) Derneryd, A.G. : Analysis of the Microstrip Disk Antenna Element, *IEEE Trans. Antennas and Propagation*, **27**, 5, (1979), pp.660-664.
13) Balanis C.A 1982 : Antenna Theory Analysis and Design, 3rd ed., John Wiley and Sons, New York., Chap.14.
14) Yu Chen, Takanori Kouno, Kazuhiro Toyoda, and Mengu Cho, Total Electron Emission of Polyimide Film Measured by a Dynamic Pulsed Scarring Method, *Applied Physics Letter*, ***99***, (2011) 152101.

Appendix

The temporal profile of :

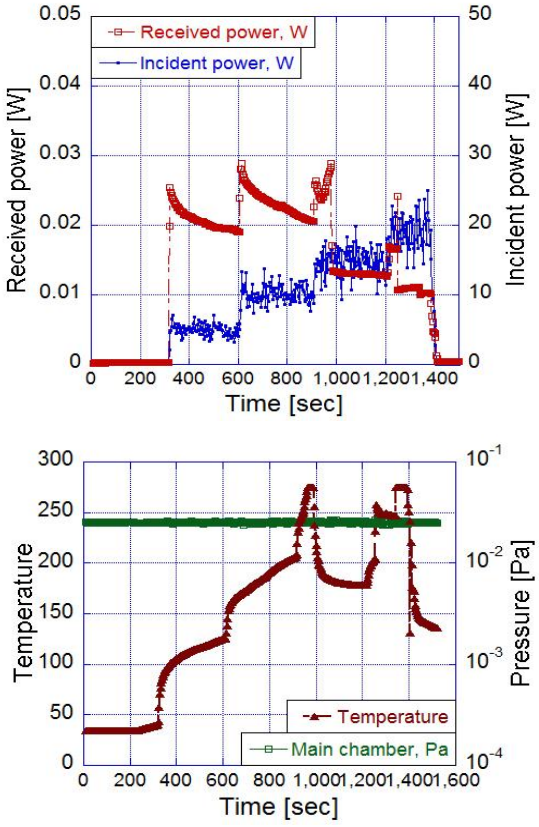

(a) Sample C

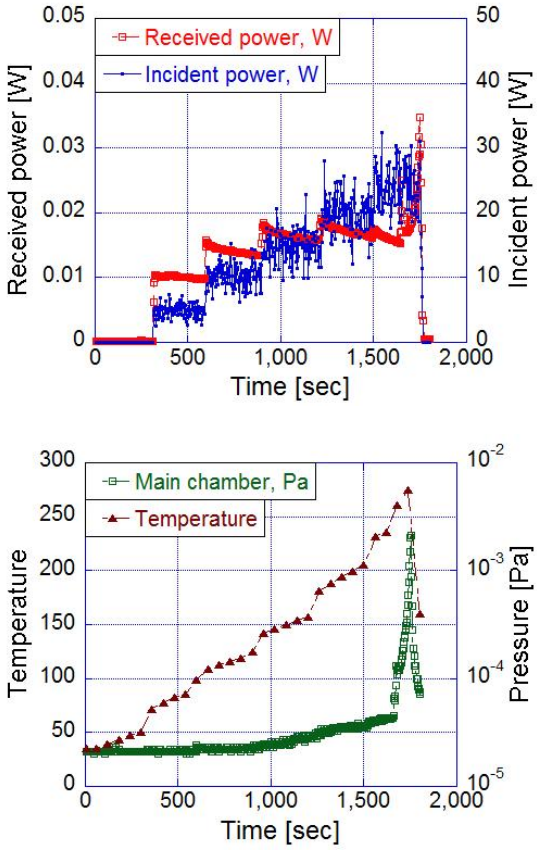

(c) Sample H

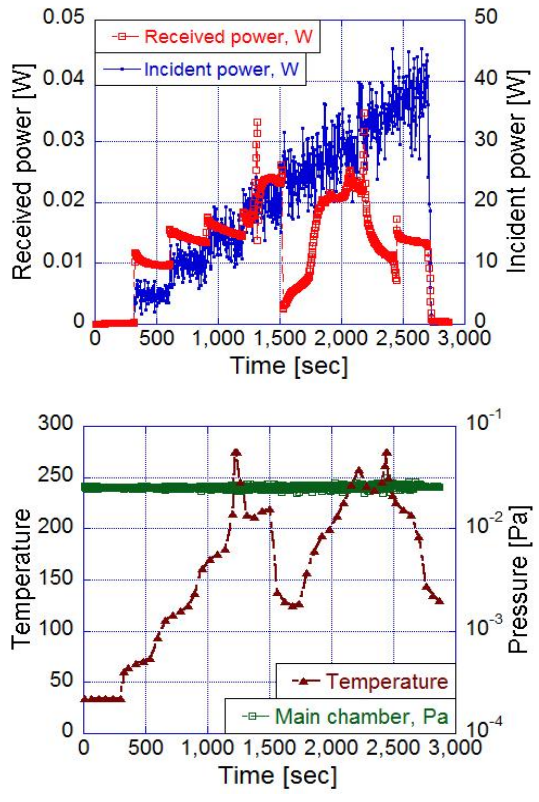

(b) Sample E

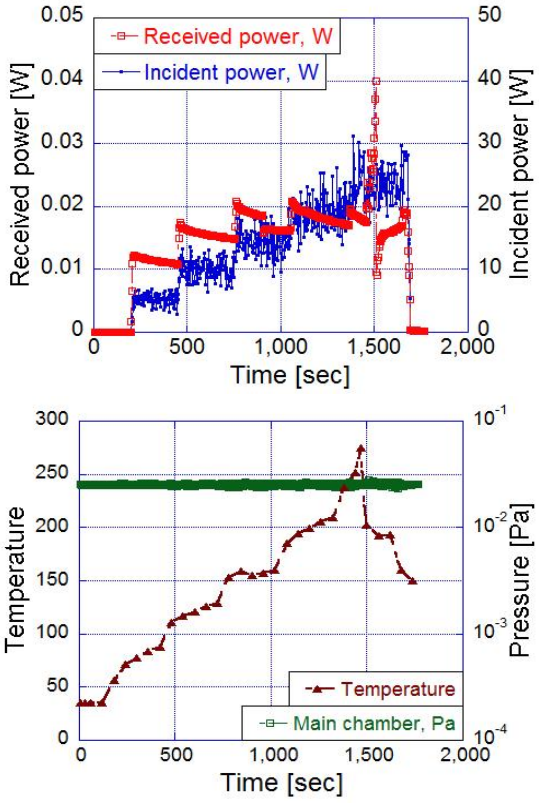

(d) Sample J